23. George, G. N. & Gorbaty, M. L. Sulfur K-edge X-ray absorption-spectroscopy of petroleum asphaltenes and models. *J. Am. Chem. Soc.* **111,** 3182–3186 (1989).
24. Gelius, U. *et al.* A new ESCA instrument with improved surface sensitivity, fast imaging properties and excellent energy resolution. *J. Electron Spectrosc. Relat. Phenom.* **52,** 747–785 (1990).
25. Puigdomenech, I. *MEDUSA* and *HYDRA*; available at ⟨http://www.inorg.kth.se/Medusa⟩ (2001).

Supplementary Information accompanies the paper on *Nature*'s website (http://www.nature.com).

Acknowledgements
We thank B. Hedman and K. O. Hodgson for support and facilities at SSRL, L. Göthe for technical assistance, and B. Lundvall at the Vasa Museum for core sampling and information. This work is supported by grants from the Knut and Alice Wallenberg Foundation, Sweden, and the Department of Energy, Office of Environmental Research (DOE-BER). SSRL is operated by the Department of Energy, Office of Basic Energy Sciences, USA.

Correspondence and requests for materials should be addressed to M.S. (e-mail: magnuss@struc.su.se).

Transient dynamics of vulcanian explosions and column collapse

A. B. Clarke*, B. Voight*, A. Neri† & G. Macedonio‡

* *Department of Geosciences, Penn State University, University Park, Pennsylvania 16802, USA*
† *Consiglio Nazionale della Ricerche, CSGSDA, Department of Earth Sciences, Pisa, Italy*
‡ *Osservatorio Vesuviano, Istituto Nazionale di Geofisica e Vulcanologia, Napoli, Italy*

Several analytical and numerical eruption models have provided insight into volcanic eruption behaviour[1–5], but most address plinian-type eruptions where vent conditions are quasi-steady. Only a few studies have explored the physics of short-duration vulcanian explosions[6–9] with unsteady vent conditions and blast events[10,11]. Here we present a technique that links unsteady vent flux of vulcanian explosions to the resulting dispersal of volcanic ejecta, using a numerical, axisymmetric model with multiple particle sizes. We use observational data from well documented explosions in 1997 at the Soufrière Hills volcano in Montserrat, West Indies, to constrain pre-eruptive subsurface initial conditions and to compare with our simulation results. The resulting simulations duplicate many features of the observed explosions, showing transitional behaviour where mass is divided between a buoyant plume and hazardous radial pyroclastic currents fed by a collapsing fountain[12]. We find that leakage of volcanic gas from the conduit through surrounding rocks over a short period (of the order of 10 hours) or retarded exsolution can dictate the style of explosion. Our simulations also reveal the internal plume dynamics and particle-size segregation mechanisms that may occur in such eruptions.

The pyroclast dispersal model[13,14] that we used, called PDAC2D, solves a set of equations expressing the conservation of mass, momentum, and energy for one gas phase and a number of solid particles of different sizes. The gas phase is a mixture of water vapour and atmospheric air, and is treated as an ideal gas. The fundamental transport equations are solved on an axisymmetric computational grid (minimum grid spacing of 5 m). The code was adapted from others originally designed for atomic explosion simulations and fluidization studies[3,4,15–17].

Information acquired on Montserrat[18] constrains input parameters, including geometries of conduit (30 m diameter) and crater (300 m diameter; 100 m depth), existence of a vent plug (estimated

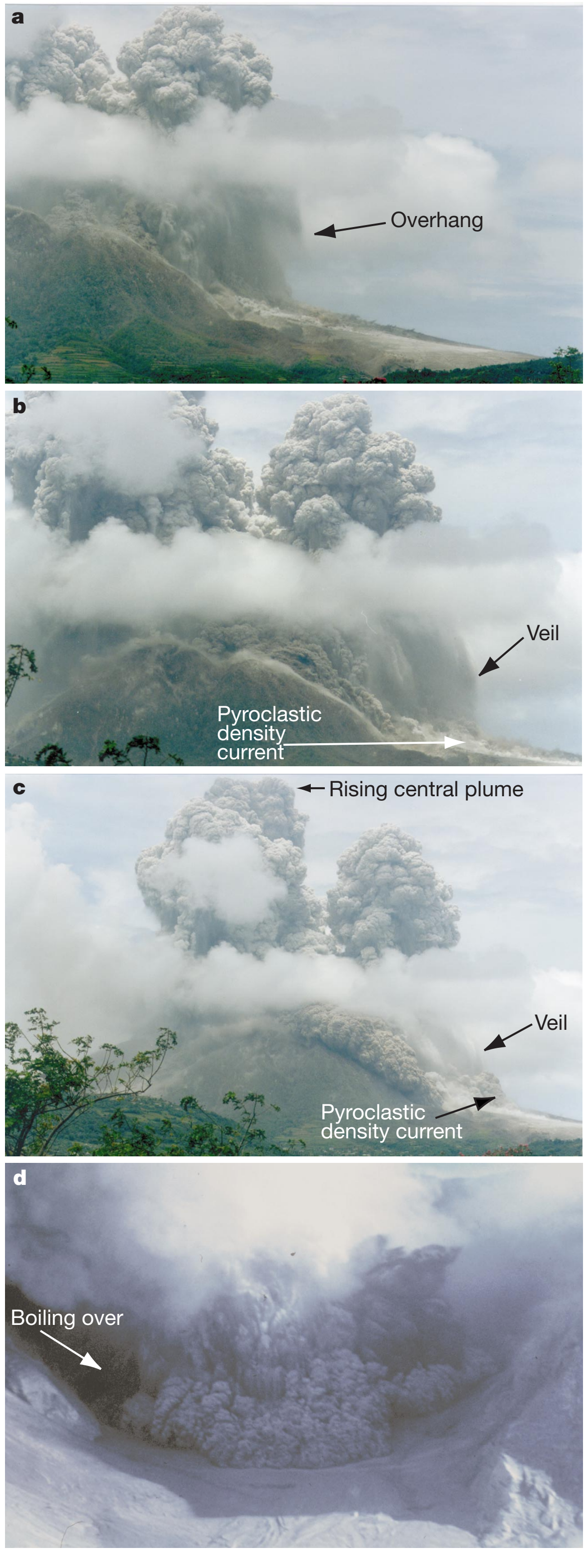

Figure 1 Examples of overhang and boil-over styles of vulcanian fountain collapse. **a**-**c**, Photographs of the 7 August 1997 vulcanian explosion of the Soufrière Hills volcano, Montserrat (by R. Herd). **a**, 25 s after onset; **b**, 32 s after onset; **c**, 35 s after onset. These photographs show fountain collapse, when the jet phase (dominated by kinetic energy) has ended and the mixture of pyroclastic debris and hot gas has not entrained sufficient air to become lighter than the surrounding atmosphere. A veil of tephra (**b** and **c**) falls from the overhanging plume; then, pyroclastic density currents, sourced from within the plume, pierce the veil and travel radially from the vent (**b** and **c**). **d**, Photograph of the eruption of Mount St Helens on 22 July 1980 (by R. Hoblitt). This is an example of the inverted-cone style of explosion where the mixture does not form an overhang and simply 'boils over' to create the pyroclastic density current.

as 20 m thick), axisymmetric topography surrounding the vent (~22° slope), and initial conduit gas pressure (10 MPa). We assume representative sizes and densities of solid particles (diameters of 30, 2,000 and 5,000 μm, representing respectively the fine and coarse particles of the conduit, and the vent plug). All solid particles have density 2,600 kg m^{-3}.

We estimate gas mass and volume fractions as functions of depth in the conduit before the explosion using conventional solubility and hydrostatic laws[19] and simple overpressure trends[20]. The dissolved water content of the chamber melt is 4.3 wt% (refs 21, 22) and the crystal volume fraction in the upper conduit, immediately before the explosions, is roughly 0.65 (petrologic studies[23] suggest about 45–55 vol.% phenocrysts (> 300 μm) and microphenocrysts (100–300 μm), and ~20 vol.% microlites (< 100 μm)). The melt phase is rhyolitic, although the bulk porphyritic rock is andesite[23]. The base of the simulation conduit ends with a solid boundary where vesicularity is 30%, corresponding to the lowest value for ejected pumice. The eruption initiates when disruption of the conduit caprock sends a fragmentation wave to a critical depth in the conduit, enabling the expanding gases to eject pyroclasts. The speed of this process far exceeds (by several orders of magnitude) the ascent rate of underlying viscous magma. However, following the

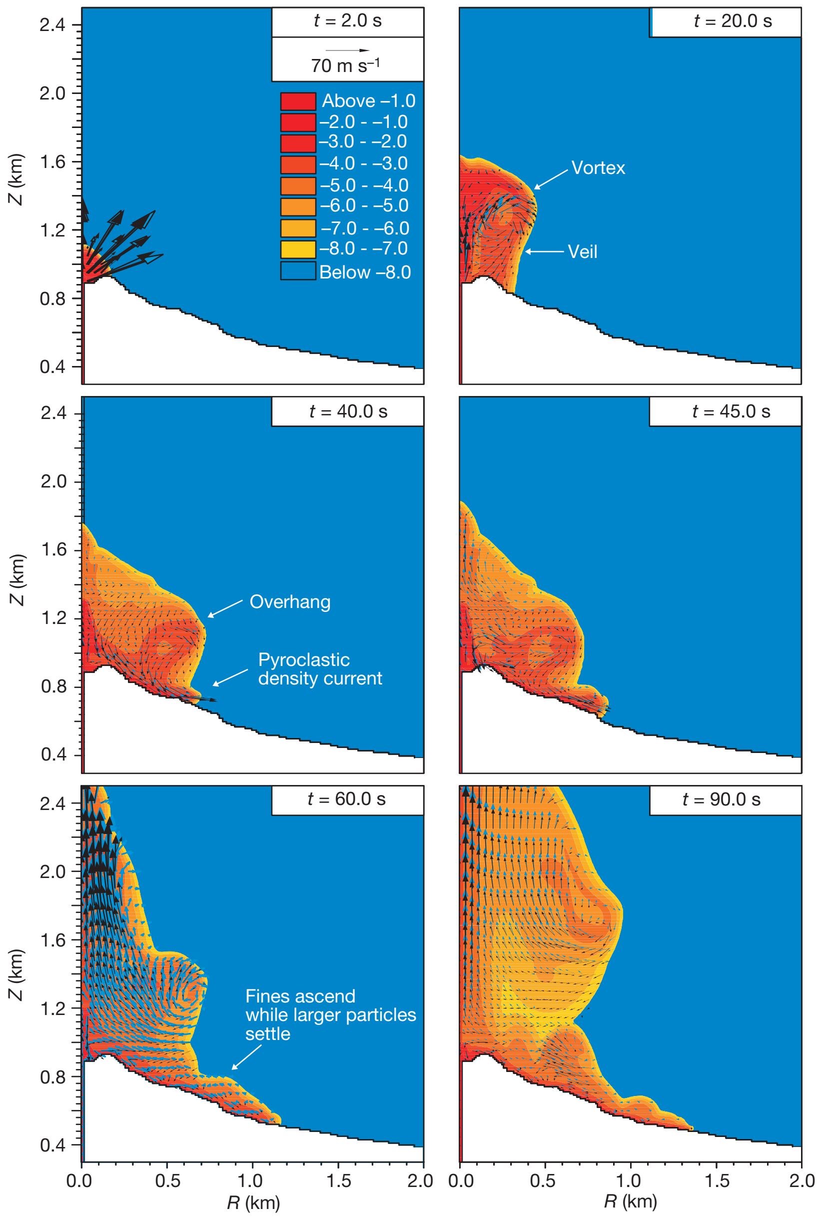

Figure 2 Particle concentration and trajectories of simulated vulcanian explosion (SimB). This series represents the development of SimB, with gas leakage (or delayed gas exsolution) intermediate between that in SimA and SimC. Input parameters were 10 MPa overpressure, constant with depth; magmatic water content 4.3 wt%; three particle sizes, namely 30, 2,000 and 5,000 μm; 10 h of volatile leakage with permeability $K = 9.0 \times 10^{-15}$ m^2. Colour contours indicate $\log_{10}$ of the total volume particle concentration in the plume, decreasing from red to yellow to blue, where −8 is the lowest visible to the naked eye. Arrows are particle velocity vectors; blue for 30 μm, black for 2,000 μm. Z is height above sea level; R is radial distance from vent. At $t = 20$ s, the clockwise vortex is centred roughly 400 m above the vent. At 40 s, the overhang (source of veil) is obvious (outer yellow region) and distinct from the annular source of the pyroclastic current. By 45 s the pyroclastic current has clearly pierced the veil. At 60 s, ascent of the central plume is greatly enhanced. At 90 s the vortex has reached more than 800 m above the vent.

explosion, a fresh batch of low-vesicularity magma rises and a new cycle of enhanced vesiculation and pressurization occurs to re-establish conditions for a potential subsequent explosion.

The three simulations discussed here are as follows: SimA, a reference simulation for which no exsolved gas leaked from the conduit before the explosion (mass ejected $M_E = 1.1\times10^9$ kg; conduit depth D_E = 1,020 m); SimB, the same as SimA after 10 h of radial leakage of volatiles through surrounding media with permeability $K_B = 9.0\times10^{-15}\,m^2$ ($M_E = 0.6\times10^9$ kg; D_E = 650 m); and SimC, the same as SimA after 10 h of leakage with $K_C = 2.7\times10^{-14}\,m^2$ ($K_C = 3\times K_B$; $M_E = 0.3\times10^9$ kg; D_E = 270 m). Volatile loss was determined by standard equations of flow through porous media[24].

These simulations support the model by predicting much of the observed behaviour, including fountain collapse height and timing, plume ascent rate through time, mass ejected, mass divided between collapsing and convective streams, generation of secondary ash plumes associated with pyroclastic currents, and pyroclastic current velocities, temperatures and runout. These correlations will be reported in detail elsewhere. Below we discuss the distinctive qualitative characteristics of two eruptive styles identified during this study, and their internal dynamics as revealed by SimA, SimB

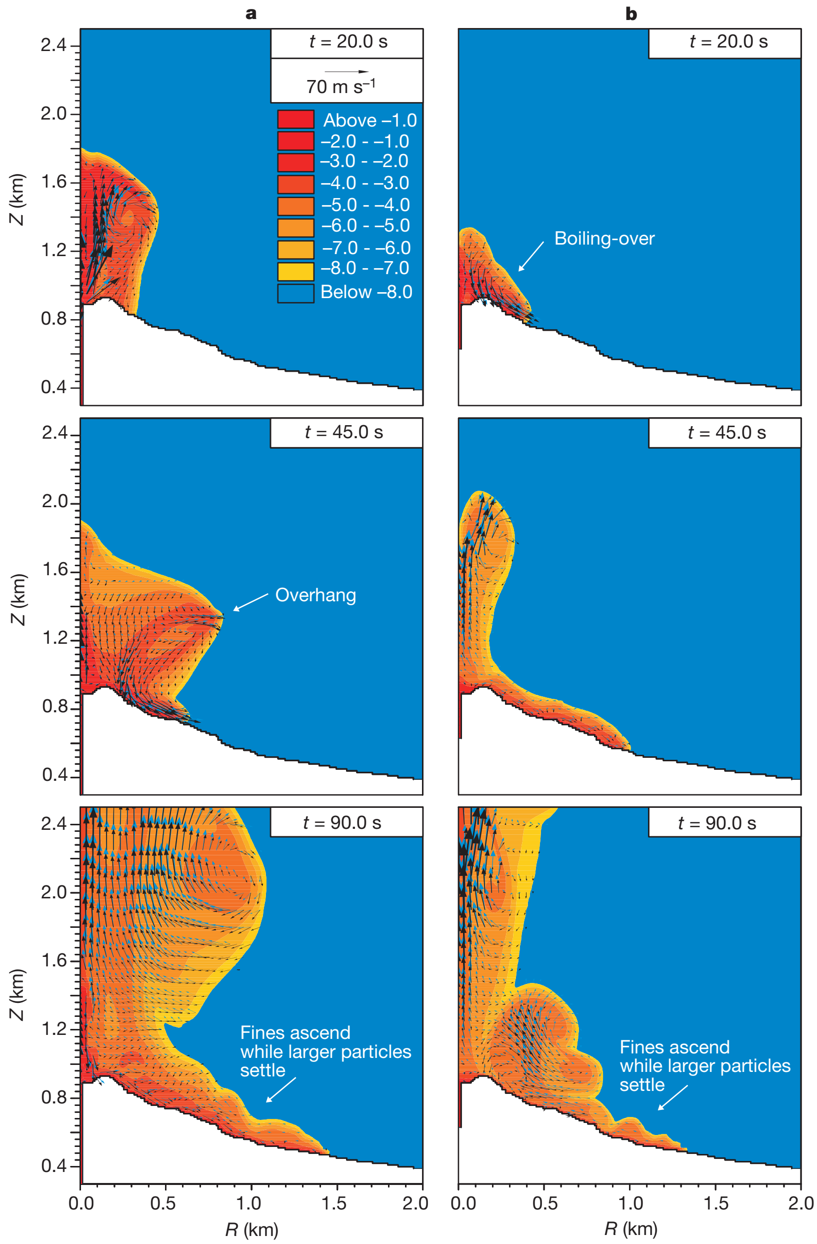

Figure 3 Particle concentrations and trajectories of simulated vulcanian explosions (SimA and SimC). Colour scale as Fig. 2. The development of SimA. Input parameters were equivalent to those of SimB but all available volatiles were allowed to participate in the simulation (no leakage). At 20 s, the clockwise vortex has developed, centred roughly 500 m above the vent. At 45 s, the pyroclastic density current has already pierced the overhanging veil. By 90 s the centre of the vortex has risen to roughly 1,200 m above the vent. **b**, The development of SimC. All input parameters of SimC are identical to those of SimB, except $K = 2.7\times10^{-14}\,m^2$ (3 times that of SimB). By 20 s, an inverted-cone-shaped region has already developed and particle velocities are parallel to the ground slope, indicating the 'boiling over' development of a pyroclastic density current. By 45 s there is a sharp distinction between the pyroclastic current and the very narrow rising plume. At 90 s, thermals, which have developed above the pyroclastic current, have moved inward and upward to join the central plume.

and SimC.

Photographs of the 7 August 1997 explosion (average mass ejected for all Montserrat events is 0.8×10^{9} kg) (Fig. 1a–c) show typical development of an overhanging plume, from which an opaque vertical veil of coarse fallout developed early in the explosion, obscuring the region under the overhang. The photographs show that the pyroclastic current did not develop from this fallout, but rather originated from a region within the plume's interior. The current subsequently pierced the opaque veil as a fast-moving, coherent, dense stream. At the same time as the emplacement of the pyroclastic current, an invigorated upward rise of the central plume occurred. Buoyant thermals also developed above the pyroclastic current[25], and subsequently joined the rapidly rising central plume. We call this style of fountain collapse the 'overhang' style. Both SimA and SimB match the qualitative characteristics of the overhang style, and therefore illustrate the internal plume processes that render the observed phenomena more understandable.

SimB (Fig. 2) represents leakage intermediate between that of SimA (Fig. 3a) and SimC (Fig. 3b). We now describe SimB (Fig. 2), which generally represents the style and development of both SimA and SimB.

The explosion begins with a nearly hemispherical expanding cap with particle velocities up to $170\,\mathrm{m\,s^{-1}}$ (Fig. 2). After 20 s, a clockwise vortex, defined mostly by fine particles (blue arrows), develops, and settling larger particles (black arrows) simulate a veil of coarse fallout outside the crater wall. By 40 s, the vortex still exists, but the inner region is dominated by downward- and outward-directed particle trajectories (mostly large particles), creating an inverted-cone-shaped region of particle sedimentation centred about the vent. Pyroclastic currents fully develop from the inverted-cone region and pierce the veil. After sedimentation associated with pyroclastic current development, the mixture becomes less dense, resulting in a rapidly rising central plume (large arrows at 60 s). Simultaneously, pyroclastic currents begin to decelerate. At 80 s (not shown), 51% of the 30-μm particles, 74% of the 2,000-μm particles, and 92% of the 5,000-μm particles are part of the density current. Partitioning of particle sizes was determined by techniques previously applied to plinian eruptions[12]. At 90 s and thereafter, the overhanging vortex continues a marked rise and thermals above the pyroclastic density current are pulled into the rising central plume. By 150 s (not shown), only 12% of the 30-μm particles remain part of the density current, reflecting removal of fine particles from the current. Velocity vectors of fine particles above the current are ventward and upward at 60 s and beyond. Also at 150 s, 77% of the 2,000-μm particles and 93% of the 5,000-μm particles are part of the current, indicating that larger particles continue to collapse. The mass distribution of SimB matches that of the real events, where approximately two-thirds of the total mass ejected entered the pyroclastic density currents.

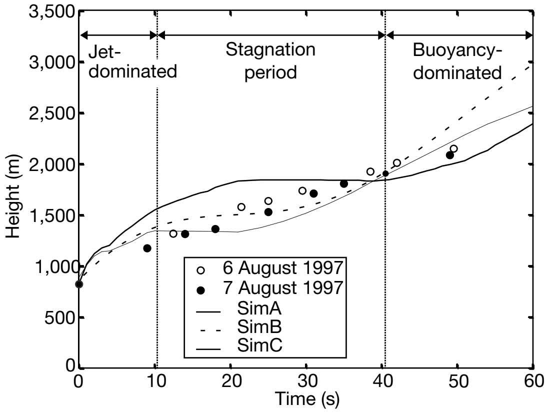

Figure 4 Comparison of real and simulated vulcanian explosions. The figure shows height versus time for SimA, SimB, SimC and two observed explosions on 6 and 7 August 1997 (data obtained from timed video). Note that SimB is generally intermediate between SimA and SimC, and most closely replicates the observed events.

In some Montserrat explosions, the initial jet rose a short distance above the vent, and within seconds an inverted-cone-shaped region of sedimentation was formed and fed pyroclastic currents. This style also occurred at Mount St Helens in July and August 1980[26] (Fig. 1d), and is akin to the 'boiling over' of gas-charged magma from an open vent, as described for Cotopaxi in 1877[27] and for Lamington in 1951[28]. SimC, which represents more extensive pre-explosion volatile leakage, reproduces this 'boil-over' (or inverted-cone) style of explosion.

By 20 s into SimC, a separation between the collapsing material and the buoyant plume is evident and pyroclastic currents begin (Fig. 3b). No overhanging plume develops, and the source of the radial pyroclastic currents is the inverted-cone-shaped region centred over the vent. The downward-directed particles in this region are primarily larger particles (black arrows). At 45 s, fine particles dominate the upper region of pyroclastic currents (blue arrows). At 60 s (not shown), 80% of the 30-μm particles, 81% of the 2,000-μm particles, and 97% of the 5,000-μm particles are part of the density current. These values are higher than those for SimB. At 90 s, a secondary thermal plume is developing above the pyroclastic current near the vent and is joining the rising central plume. The percentage of 30-μm particles in the collapsed mixture is reduced to 57% by this thermal, while the fractions of the 2,000- and 5,000-μm particles remain the same as they were at 60 s.

In general, the overhang style occurs for initial conditions with little or no volatile depletion, whereas the boil-over style occurs for cases with lower volatile fraction. The boil-over style tends to emplace a greater fraction of the total mass erupted as pyroclastic density currents than does the overhang style. As expected, fountain collapse heights and times are inversely related to the amount of leakage of conduit volatiles. The finest particles are removed from the pyroclastic currents by rising thermals for both styles, with the overhang style exhibiting the more marked effect.

In Fig. 4, the temporal variation of the simulated plume height above the vent is compared against data (based on timed video) for two 1997 vulcanian explosions. The plume height and vertical velocity trends of the simulations follow qualitatively those of the 6 and 7 August explosions—but the simulations produce minimum ascent velocities less than those measured. This may reflect the multiple-jet character of the real explosions[29] that incrementally added heat and turbulence to the complex plumes. Our simulations do not attempt to account for this phenomenon.

SimA exhibits the most energetic plume development, consistent with its zero volatile leakage. SimB and SimC, both with lateral volatile leakage, match the observed ascent rates rather well, whereas SimB also reproduces the overhang style observed, making it our best match for the 6 and 7 August events. This good correspondence suggests that leakage of volatiles from the conduit system and/or retarded exsolution may have controlled the Montserrat vulcanian explosions, and that the internal dynamics of our simulations are probably similar to the internal dynamics of the real explosions.

Our study shows the importance of volatile leakage from the pre-explosion conduit in dictating not only the energy of an explosion but also the style of fountain collapse, with two different types identified and named. A more complex volatile description is therefore planned for future simulations[24,30]. Our results demonstrate that multi-phase numerical models can duplicate many features of highly complex natural eruptions, and can illuminate internal dynamics that cannot be observed by ordinary means: such models are therefore valuable tools in hazard mitigation. □

Received 9 October 2001; accepted 17 January 2002.

1. Sparks, R. S. J., Wilson, L. & Hulme, G. Theoretical modeling of the generation, movement, and emplacement of pyroclastic flows by column collapse. *J. Geophys. Res.* **83,** 1727–1739 (1978).
2. Valentine, G. A. & Wolhletz, K. H. Numerical models of Plinian eruption columns and pyroclastic flows. *J. Geophys. Res.* **94,** 1867–1887 (1989).
3. Dobran, F., Neri, A. & Macedonio, G. Numerical simulation of collapsing volcanic columns. *J. Geophys. Res.* **98,** 4231–4259 (1993).
4. Neri, A. & Macedonio, G. Numerical simulation of collapsing volcanic columns with particles of two sizes. *J. Geophys. Res.* **101,** 8153–8174 (1996).
5. Oberhuber, J. M., Herzog, M., Graf, H. F. & Schwanke, K. Volcanic plume simulation on large scales. *J. Volcanol. Geotherm. Res.* **87,** 29–53 (1998).
6. Self, S., Wilson, L. & Nairn, I. A. Vulcanian eruption mechanisms. *Nature* **277,** 440–443 (1979).
7. Turcotte, D. L., Ockendon, H., Ockendon, J. R. & Cowley, S. J. A mathematical model of Vulcanian eruptions. *Geophys. J. Int.* **103,** 211–217 (1990).
8. Fagents, S. A. & Wilson, L. Explosive volcanic eruptions—VII. The ranges of pyroclastics ejected in transient volcanic explosions. *Geophys. J. Int.* **113,** 359–370 (1993).
9. Woods, A. W. A model of Vulcanian explosions. *Nucl. Eng. Des.* **155,** 345–357 (1995).
10. Kieffer, S. W. Fluid dynamics of the May 18 blast at Mount St. Helens. *US Geol. Surv. Prof. Pap.* **1250,** 379–400 (1981).
11. Wohletz, K. H., McGetchin, T. R., Sandford, M. T. & Jones, E. M. Hydrodynamic aspects of caldera-forming eruptions: numerical models. *J. Geophys. Res.* **89,** 8269–8285 (1984).
12. Neri, A., Di Muro, A. & Rosi, M. Mass partition during collapsing and transitional columns by using numerical simulations. *J. Volcanol. Geotherm. Res.* (in the press).
13. Neri, A. *Multiphase Flow Modelling and Simulation of Explosive Volcanic Eruptions.* Thesis, Illinois Inst. Technol. (1998).
14. Neri, A., Macedonio, G., Gidaspow, D. & Esposti Ongaro, T. *Multiparticle Simulation of Collapsing Volcanic Columns and Pyroclastic Flows* (Volcanic Simulation Group Report 2001–2, Instituto Nazionale di Geofisica e Vulcanologia, Pisa, 2001).
15. Amsden, A. A. & Harlow, F. H. *KACHINA: An Eulerian Computer Program for Multifield Fluid Flows* (Report LA-5680, Los Alamos National Laboratory, Los Alamos, 1974).
16. Rivard, W. C. & Torrey, M. D. *K-FIX: A Computer Program for Transient, Two-dimensional, Two-fluid Flow* (Report LA-NUREG-6623, Los Alamos National Laboratory, Los Alamos, 1977).
17. Gidaspow, D. *Multiphase Flow and Fluidization: Continuum and Kinetic Theory Descriptions* (Academic, New York, 1994).
18. Voight, B. *et al.* Magma flow instability and cyclic activity at Soufrière Hills Volcano, Montserrat. *Science* **283,** 1138–1142 (1999).
19. Wilson, L., Sparks, R. S. J. & Walker, G. P. L. Explosive volcanic eruptions IV. The control of magma properties and conduit geometry on eruption column behaviour. *Geophys. J. R. Astron. Soc.* **63,** 117–148 (1980).
20. Sparks, R. S. J. Causes and consequences of pressurisation in lava dome eruptions. *Earth Planet. Sci. Lett.* **150,** 177–189 (1997).
21. Devine, J. D., Rutherford, M. J. & Barclay, J. Changing magma conditions and ascent rates during the Soufrière Hills eruption on Montserrat. *GSA Today* **8,** 2–7 (1998).
22. Barclay, J. *et al.* Experimental phase equilibria constraints on pre-eruptive storage conditions of the Soufrière Hills magma. *Geophys. Res. Lett.* **25,** 3437–3440 (1998).
23. Murphy, M. D., Sparks, R. S. J., Barclay, J., Carroll, M. R. & Brewer, T. S. Remobilization of andesite magma by intrusion of mafic magma at the Soufrière Hills Volcano, Montserrat, West Indies. *J. Petrol.* **41,** 21–42 (2000).
24. Jaupart, C. & Allègre, C. J. Gas content, eruption rate and instabilities of eruption regime in silicic volcanoes. *Earth Planet. Sci. Lett.* **102,** 413–429 (1991).
25. Druitt, T. H. *et al. The Explosive Eruptions of August 1997* (Special Report 04, Montserrat Volcano Observatory, Salem, Montserrat, 1998).
26. Hoblitt, R. P. Observations of the eruptions of July 22 and August 7 1980 at Mount St Helens, Washington. *US Geol. Surv. Prof. Pap.* **1335,** (1986).
27. Wolf, T. Der Cotopaxi und seine letzte Eruption am 26 Juni 1877. *Neues Jb. Miner. Geol. Paläont.* 113–167 (1878).
28. Taylor, G. A. The 1951 eruption of Mount Lamington, Papua. *Aust. Bur. Min. Resour. Geol. Geophys. Bull.* **38,** 1–117 (1958).
29. Formenti, Y. & Druitt, T. H. in *Abstracts and Addresses of the IAVCEI General Assembly 2000* 232 (Volcanological Survey of Indonesia, Bandung, Indonesia, 2000).
30. Melnik, O. & Sparks, R. S. J. Nonlinear dynamics of lava dome extrusion. *Nature* **402,** 37–41 (1999).

Acknowledgements

We thank our colleagues at Montserrat Volcano Observatory for their assistance, especially C. Bonadonna, T. Druitt, C. Harford, R. Herd, R. Luckett and R.E.A. Robertson, our colleagues during the August explosions. Support for monitoring was provided by the Department for International Development (UK), the British Geological Survey (BGS), the Seismic Research Unit of the University of the West Indies, and the US Geological Survey (USGS). A.C. and B.V. acknowledge support from the US NSF. A.N. and G.M. were assisted by the Istituto Nazionale di Geofisica e Vulcanologia, and Gruppo Nazionale per la Vulcanologia INGV, Italy. B.V. was a Senior Scientist at Montserrat in 1997 with BGS, and was also affiliated with the USGS Volcano Hazards Program. We thank M. Rutherford for comments.

Competing interests statement

The authors declare that they have no competing financial interests.

Correspondence and requests for materials should be addressed to A.B.C. (e-mail: aclarke@geosc.psu.edu).